Published OnlineFirst April 15, 2013; DOI: 10.1158/1078-0432.CCR-12-3947

Human Cancer Biology

Clinical Cancer Research

Early Telomere Shortening and Genomic Instability in Tubo-Ovarian Preneoplastic Lesions

Gautier Chene[1,2,3,4], Andrei Tchirkov[2], Eleonore Pierre-Eymard[2], Jacques Dauplat[3], Ines Raoelfils[1], Anne Cayre[1], Emmanuel Watkin[5], Philippe Vago[2], and Frederique Penault-Llorca[1]

Abstract

Purpose: Genetic instability plays an important role in ovarian carcinogenesis. We investigated the level of telomere shortening and genomic instability in early and preinvasive stages of ovarian cancer, serous tubal intraepithelial carcinoma (STIC), and tubo-ovarian dysplasia (TOD).

Experimental Design: Fifty-one TOD from prophylactic salpingo-oophorectomies with *BRCA1* or *2* mutation, 12 STICs, 53 tubo-ovarian high-grade serous carcinoma, and 36 noncancerous controls were laser capture microdissected from formalin-fixed, paraffin-embedded sections, analyzed by comparative genomic hybridization (array CGH) and for telomere length (using quantitative real-time PCR based on the Cawthon's method). TOD and STICs were defined by morphologic scores and immunohistochemical expressions of p53, Ki67, and γH2AX.

Results: TOD showed marked telomere shortening compared with noncancerous controls ($P < 10^{-7}$). STICs had even shorter telomeres than TOD ($P = 0.0008$). Ovarian carcinoma had shorter telomeres than controls but longer than STICs and dysplasia. In TOD, telomeres were significantly shorter in those with BRCA1 mutation than in those with BRCA2 mutation ($P = 0.005$). In addition, γH2AX expression in TOD and STIC groups with short telomeres was significantly increased ($P < 10^{-7}$). In dysplastic epithelium, we found subtle genomic alterations, in contrast to more important genomic imbalances in STICs. The total number of genetic alterations was the highest in ovarian cancers.

Conclusions: These findings suggest that genetic instability occurs in early stages of ovarian tumorigenesis. STICs and noninvasive dysplasia are likely an important step in early serous ovarian neoplasia. *Clin Cancer Res; 19(11); 2873–82. ©2013 AACR.*

Introduction

Ovarian serous cancer is the most life-threatening gynecologic malignancy. A better understanding of the molecular basis of the disease and the preinvasive stages would be helpful for defining means of prevention or early detection. Genetic instability is one of the characteristics shared by most human cancers and seems to exist (at various levels) at all stages of the disease, from precancerous lesions to advanced cancer. It is possible that this instability is one of the first trigger events which would facilitate the subsequent establishment of all the other cancer hallmarks (1, 2).

Recent meticulous and exhaustive histopathologic analysis of specimens from prophylactic adnexectomy in BRCA gene mutation carriers revealed in up to 17% of patients occult cancers, 57% to 100% of which were located in the distal portion of the tubes (called serous tubal intraepithelial cancer or STIC; refs. 3–8). Similar lesions have also been revealed in series of sporadic ovarian or peritoneal cancer, suggesting that serous ovarian carcinogenesis could have a tubal origin. In the serous ovarian carcinogenic sequence, histopathologic anomalies termed tubal dysplasias (or tubal intraepithelial lesions in transition: TILT or p53 proliferation signature) along with ovarian anomalies have been described and could precede STIC lesions (9–13). They are characterized by cytologic and architectural abnormalities (see Materials and Methods), an overexpression of p53, a low proliferation index (Ki67 between 10% and 40%), and evidence of DNA damage manifested by immunopositivity for H2AX. Nonproliferative p53 signatures are earlier entities. They exhibit no abnormal histologic features and have an immunohistochemical definition with at least 12 consecutive secretory cells that are p53-positive and have a low proliferation index (Ki67 < 10%). They have also evidence of DNA damage by staining with γH2AX (14).

In the present study, we examined the genetic instability of these probably precancerous tubo-ovarian lesions at

Authors' Affiliations: [1]Department of Histopathology, Centre Jean Perrin, ERTICA Research Team, [2]Department of Cytogenetics, CHU Clermont-Ferrand; ERTICA Research Team, University of Auvergne; [3]Department of Surgery, Centre Jean Perrin, Clermont-Ferrand; [4]Department of Obstetric, Gynecology & Reproductive Medicine, CHU St Étienne, Saint-Étienne; and [5]Department of Histopathology, Croix-Rousse Hospital, Lyon, France

Note: Supplementary data for this article are available at Clinical Cancer Research Online (http://clincancerres.aacrjournals.org/).

Corresponding Author: Gautier Chene, Department of Surgery, Centre Jean Perrin, 58 rue Montalembert, Clermont-Ferrand, 63000, France. Phone: 33-6-07-08-17-86; Fax: 33-4-77-82-89-56; E-mail: chenegautier@yahoo.fr

doi: 10.1158/1078-0432.CCR-12-3947

©2013 American Association for Cancer Research.

Downloaded from clincancerres.aacrjournals.org on September 20, 2020. © 2013 American Association for Cancer Research.

Published OnlineFirst April 15, 2013; DOI: 10.1158/1078-0432.CCR-12-3947

Translational Relevance

The study of genomic instability in tubo-ovarian precancerous lesions could have important implications in the understanding and the early diagnosis of serous ovarian carcinoma.

three different levels. First, by analyzing the telomere length, as the telomere dysfunction has been described as one of the early events contributing to genomic instability (15–17).

In addition, we studied the activation of the DNA damage response in STICs and in precursor lesions using immunohistochemical detection of H2AX phosphorylation.

Finally, we investigated the presence of chromosomal rearrangements in these early lesions.

Material and Methods

Patients

This retrospective study was conducted on tissue samples provided by the Pathology Departments of the Jean Perrin Anticancer Center (Clermont-Ferrand, France) and Croix-Rousse Hospital (Lyon, France) and obtained in 3 patient and 1 control groups

- Dysplasia: A total of 51 cases (20 ovarian and 31 tubal dysplasias) obtained after 36 prophylactic adnexectomies in *BRCA1* gene carriers and 15 prophylactic adnexectomies in *BRCA2* gene carriers.
- STICs: Twelve cases, none of these have a BRCA mutation.
- Cancer: Fifty-three high-grade serous tubo-ovarian cancers (16 cancers of tubal and 37 cancers of ovarian origin).
- Controls: Thirty-six adnexectomies in a spontaneously fertile woman with no personal nor family history of gynecologic cancer (breast, ovary, endometrium) for which histopathology concluded that the ovaries were free of any cancerous or borderline pathology.

The review board of the Jean Perrin Anticancer Center approved all experimental research reported in this study.

Histopathological criteria

We defined the cases of ovarian and tubal dysplasia on the basis of the morphologic and immunohistochemical criteria described recently in the literature (9, 10, 14, 18–21). In brief, ovarian dysplasia was defined by the following morphologic features: epithelial multilayering, tufting, surface papillomatosis, nuclear chromatin irregularity, nuclear contour irregularity, cellular pleomorphism, increased nuclear size, epithelial inclusion cysts, psammoma bodies, deep cortical invaginations, and cortical stromal hyperplasia. Tubal dysplasia was defined by the following morphologic dysplasia: epithelial multilayering, tufting, loss of nuclear polarity, increase in nuclear density, nuclear atypia, increased nuclear size, and loss of ciliation. Both tubal and ovarian dysplasia had p53 expression, low Ki67 proliferative index, and immunopositivity for γH2AX.

The diagnosis of STICs complied with the criteria of Kuhn and colleagues (22): nonciliated cells exhibiting 3 or more of the following features: (i) abnormal chromatin pattern, (ii) nuclear enlargement, (iii) marked nuclear pleomorphism, (iv) epithelial stratification and/or loss of polarity, and (v) nuclear molding.

The diagnosis of primary carcinoma of the tube complied with the criteria established by Hu and Sedlis (23, 24).

An immunohistochemical analysis of p53 and Ki67 was carried out (respectively DAKO, DO-7, 1:200 and DAKO, MIB-1, 1:100) to help with the diagnosis of tubo-ovarian dysplasia (TOD) and STICs. In addition, γH2AX (Millipore, JBW301, 1:50) was used on 3-mm paraffin sections on dry silanized slides for one night at 56°C. In brief, antibody staining was carried out in a Benchmark XT and revealed using the Ultraview DAB kit (Roche Ventana).

Semiquantitative assessment (quick score) of γH2AX was made by 2 pathologists (IR/FPL) using an optical microscope.

Laser microdissection and DNA extraction

We used a PixCell II (Artcurus) microdissection system, which allows laser microdissection of cells of interest to be made from paraffin sections (10 consecutive sections each of 14 μm) according to the manufacturer's protocol. Briefly, the cells examined (morphologically dysplastic epithelial cells in group A, cancerous cells in groups group in C, and epithelial cells of normal appearance in control group D) initially with a Nikon TiE Inverted microscope were microdissected (the surrounding tissue remaining intact on the slide) and adhered to the film when the capsule was lifted away from the tissue. The capsule was then placed in a microtube containing the cell lysis solution to extract the DNA (25, 26).

We used the PicoPure DNA (Arcturus) extraction kit to extract the genomic DNA from the microdissected cells, followed by a purification step (QIAamp DNA Mini Kit, Qiagen).

The DNA concentration was established by spectrophotometry (Nanodrop, Nanodrop Technologies).

DNA yields and quality were within the same range.

Quantification of telomere length using quantitative real-time PCR

The telomere length measurement assay was adapted from the published original quantitative real-time PCR (qRT-PCR) method (27, 28). This method measures the relative average telomere lengths in gDNA by determining the ratio of telomere repeat copy number to single gene copy number (T/S ratio) in experimental samples relative to a reference sample. Previously, it has been shown that the results obtained using this method correlate very well with results of classical terminal restriction fragment (TFR) length by Southern blot technique (27, 28). Telomere repeated sequences and glyceraldehyde-3-phosphate dehydrogenase gene (*GAPDH*) amplification was carried out for each DNA sample by real-time PCR. *GADPH* was used as

Downloaded from clincancerres.aacrjournals.org on September 20, 2020. © 2013 American Association for Cancer Research.

Published OnlineFirst April 15, 2013; DOI: 10.1158/1078-0432.CCR-12-3947

single-copy gene control (S). Primers were as follows: for *GAPDH*, forward CCCCACACACATGCACTTACC and reverse CCTAGTCCCAGGGCTTTGATT (29); for telomeric DNA, forward ACACTAAGGTTTGGGTTTGGGTTTGGGTT-TGGGTTAGTGT and reverse TGTTAGGTATCCCTATCCC-TATCCCTATCCCTATCCCTAACA (28). PCR amplification was conducted in the LightCycler 480 Real-Time PCR system (Roche Diagnostics) using the LightCycler 480 SYBR Green Master Kit (Roche Diagnostics). Both telomere and single-copy gene amplifications were conducted on each DNA sample (10 ng) on the same reaction plate, and amplifications were carried out under the same PCR conditions to eliminate the interplate variation. Thermal cycling was carried out according to the following protocol: 95°C for 10 minutes to activate Taq polymerase, followed by 35 cycles of 95°C for 10 seconds, 62°C for 15 seconds, and 72°C for 15 seconds. A melting (dissociation) curve was generated on every run to confirm the specificity of the reaction.

The amplification efficiency for both *GAPDH* and telomere DNA was examined with a set of serial dilutions of a reference human DNA (a pooled normal blood DNA samples from 5 healthy donors) and found to be >90% with correlation coefficients of $\geq$99% for both primer sets. The ΔC_t (threshold cycle number) method was used for the calculation of T/S ratios. All samples were measured at least in duplicate.

Array comparative genomic hybridization

We made a high-resolution array comparative genomic hybridization (aCGH) study using oligonucleotide microarrays (Agilent 180 K) of 10 adnexectomies in dysplasia group, 12 STICs, and 15 high-grade serous ovarian cancers compared with a control DNA extracted either from ovary or fallopian tube and free of any infectious or cancerous pathology. We deliberately studied with aCGH the most characteristic at morphologic and immunohistochemical levels dysplastic cases from the subgroup carrying BRCA1 mutations.

We used a 180K CGH oligonucleotide microarray (Agilent Technologies). Each case was hybridized twice, marked once with Alexa 3 and once with Alexa 5 in the DNA mixtures during hybridization.

Briefly, 1 to 2 μg of purified DNA (sample and sex-matched reference) was chemically labeled respectively with 25 μL d'Alexa Fluor 3 Oligo aCGH 2X Reaction Mix and Alexa Fluor 5 Oligo aCGH 2X Reaction Mix at 37°C for 120 minutes according to the manufacturer's instructions (Bioprime Total Genomic Labelling Kit, Invitrogen). Labeled samples were purified (Purification Module B with Pure link, Invitrogen), mixed with human Cot-1 DNA and denatured at 95°C (Oligo aCGH hybridization kit). The mixture was applied to microarrays and hybridization was conducted at 65°C for 24 hours. After hybridization, the microarrays were washed in Oligo aCGH wash buffer 1 at room temperature for 5 minutes and wash buffer 2 at 37°C for 1 minute. After drying, the microarrays were scanned using a DNA microarray scanner G2565BA (Agilent) and data ($\log_2$) were extracted from raw microarray image files using Feature Extraction software (version 9.2, Agilent). Then, data were analyzed by DNA Analytics software (version 3.4, Agilent) with default filter settings: this software allows a dye-flip analysis, taking $\log_2$ ratios > or <0.25 and −0.25 for 3 consecutive spots as thresholds for the detection of a copy number gain and loss, respectively.

Areas with less than 3 consecutive spots and that were not confirmed by dye-flip analysis in the 2 tests were eliminated.

The altered chromosomal regions were then checked using databases: UCSC Genome Browser and the database developed by the Western France genomic center at Nantes (http://cardioserve.nantes.inserm.fr/madtools/home/).

Finally, the results were compared with known polymorphic CNVs (Database of Genomic Variants). The nonpolymorphic regions of each case were then listed, i.e. the

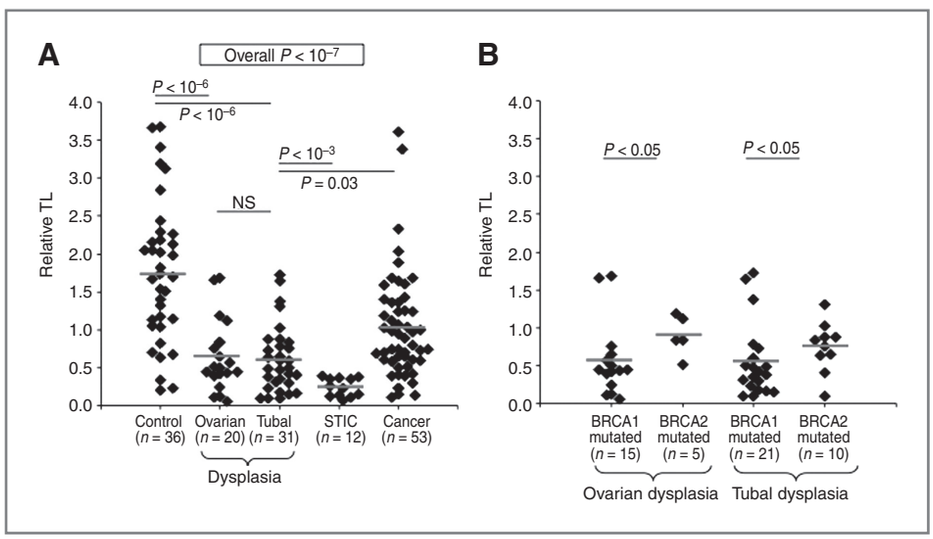

Figure 1. Individual and mean values of relative telomere length (TL) in investigated groups. The statistical comparison was carried out using the Kruskal–Wallis *H* test. A, significant differences in telomere length between normal tubal/ovarian tissue and samples obtained from ovarian/tubal dysplasia, STICs, and tubo-ovarian cancer. B, shorter telomeres in BRCA1-mutated ovarian and tubal dysplasia cases than in BRCA2-mutated cases.

Downloaded from clincancerres.aacrjournals.org on September 20, 2020. © 2013 American Association for Cancer Research.

Published OnlineFirst April 15, 2013; DOI: 10.1158/1078-0432.CCR-12-3947

regions found with a ratio > 0.58 [log (2) 3/2] or <−1 [log (2) 1/2], for 3 consecutive nonpolymorphic spots.

Each of the arrays was independently analyzed and evaluated for genetic alterations.

Statistical analysis

Molecular analysis of the results by CGH array was descriptive (small cohort).

Telomeric and immunohistochemical parameters obtained in different groups were compared with nonparametric Wilcoxon or Kruskal–Wallis *H*-tests. The relationship between variables was tested using Pearson correlation analysis.

Results

Telomere lengths and immunohistochemical analysis

The T/S ratio obtained for each sample reflects the relative telomere length. We compared the T/S values between control, dysplasia, STIC, and cancer groups. In addition, we evaluated the impact of genetic characteristics (BRCA1 and BRCA2 status) and expression of p53 and γH2AX proteins.

Across the groups, the mean telomere length differed significantly (Fig. 1). Dysplasia group showed telomere shortening, as compared to the controls. Telomeres were even shorter in STICs. Interestingly, cancer group showed longer telomeres than dysplasia and STIC cases but shorter than those of the control group. No significant difference was found depending on the type of organ (ovary or tube) whether for the control, dysplasia, or cancer cases (Table 1). However, the telomere length was significantly altered in case of BRCA mutation ($P = 0.005$): T/S ratio = 0.56 in case of BRCA1 mutation versus 0.80 in case of BRCA2 mutation, so the telomere length was shorter in subgroup BRCA1.

Regarding immunohistochemical characteristics (Figs. 2 and 3), the expression of γH2AX was significantly higher in case of dysplasia and STICs than in cancers (Fig. 2A, $P < 10^{-7}$). There was a significant inverse correlation (Fig. 2C, $P = 0.00013$) between γH2AX expression and telomere length: telomeres were shorter in cases with higher levels of γH2AX. The level of p53 expression was higher in STIC and cancer groups compared to dysplasia group (Fig. 2B, $P < 10^{-7}$). Within dysplasia and STIC groups, the level of p53 correlated inversely with the telomere length (Fig. 2D, $P = 0.0016$). Of note, the level of p53 was homogenously and highly (mean score near 100%) elevated in cancers. The Ki-67 labeling showed high levels in cancer (81.0% ± 4.9%) and STIC (52.5% ± 16.3%) groups, whereas the values seen in ovarian (6.4% ± 4.7%) and tubal dysplasia (8.0% ± 6.3%) were much lower and not different from each other. There was a highly significant difference between the 3 groups: cancer, STIC, and dysplasia ($P < 10^{-6}$, *H* test).

aCGH

Among the 10 adnexectomies in the dysplasia group with genetic risk, it was possible to study only 5 ovaries and 9 tubes due to insufficient material. Twelve STICs and 15 high-grade serous ovarian cancers were also analyzed. The most common changes found in these subgroups are shown in Fig. 3 and detailed in Supplementary Tables S1–S3.

aCGH results for tubo-ovarian dysplasia samples. Both DNA copy number gains and losses were found (Figs. 4 and 5). The mean number of genomic changes was 4.25 (2–7) in ovaries and 6.5 (4–11) in tubes. The most common gains were detected in tubes at chromosomes 4q (6 of 9 cases, 66.6%), 6q (2 of 9, 22.2%), 14q (2 of 9, 22.2%), 20q (2 of 9, 22.2%), and 3q (1 of 9, 11.1%). No common gain was found in ovaries. The most common DNA copy number losses were detected in tubes at chromosomes 1p (5 of 9, 55.5%), 15q (5 of 9, 55.5%), 6p (4 of 9, 44.4%), 8p (4 of 9, 44.4%), 11q (4 of 9, 44.4%), 12q (4 of 9, 44.4%), 12 p (4 of 9, 44.4%), and 1q (3 of 9, 33.3%). In ovaries, common losses involved chromosomes 1q (2 of 5, 40%), 8p (2 of 5, 40%), 14q (2 of 5, 40%), and 15q (2/5, 40%).

The mean size of rearrangements was 404.44 kb (72–1318) for ovarian dysplasia and 758.85 kb (44–6452) for tubal dysplasia cases. The minimal regions of interest in the

Table 1. The relative telomere length in normal dysplastic and cancerous tubal/ovarian epithelium

		Relative telomere length		
Group	No. of samples	Mean (SEM)	*P* (ovary vs. tube)	*P* (dysplasia, STIC, cancer vs. control ovary or tube)
Control				
Ovary	12	1.892 (0.20)	0.56 (NS)	—
Tube	24	1.691 (0.21)		—
Dysplasia				
Ovary	20	0.647 (0.10)	0.77 (NS)	0.00012
Tube	31	0.613 (0.08)		0.000013
STIC	12	0.241 (0.11)	—	0.0000087
Cancer				
Ovary	37	1.168 (0.24)	0.92 (NS)	0.000023
Tube	16	0.953 (0.09)		0.046

Abbreviations: SEM, standard error of the mean; NS, not significant.

Downloaded from clincancerres.aacrjournals.org on September 20, 2020. © 2013 American Association for Cancer Research.

Published OnlineFirst April 15, 2013; DOI: 10.1158/1078-0432.CCR-12-3947

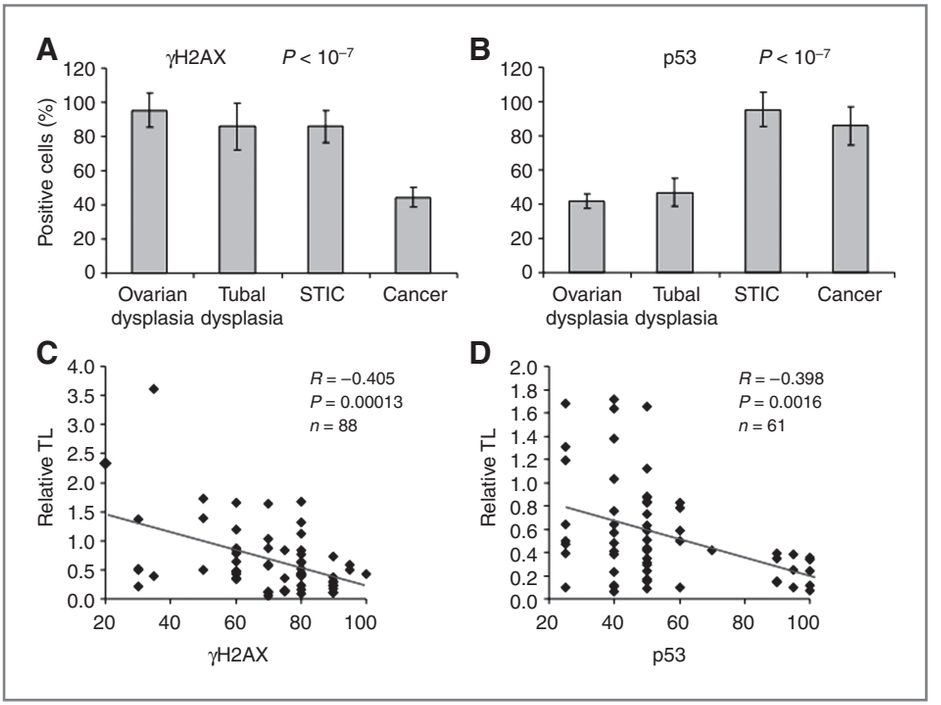

Figure 2. A, elevated γH2AX levels detected with immunochemistry in ovarian ($n = 18$) and tubal ($n = 27$) dysplasia and STIC ($n = 12$) compared with cancer cases ($n = 27$). B, the score of p53 staining was significantly higher in STICs ($n = 12$) and cancer ($n = 52$) groups than in ovarian ($n = 18$) and tubal ($n = 27$) dysplasia groups. C, significant inverse correlation between the level of γH2AX expression and telomere length (TL) observed in cases of dysplasia, STICs, and cancer ($n = 88$). D, significant inverse correlation between the level of p53 expression and telomere length in dysplasia and STICs ($n = 61$).

common losses and gains are presented in Supplementary Tables S1 and S2.

aCGH results for STIC samples. The mean number of rearrangements was greater than in dysplasia cases (8.6, 4–17; Fig. 4). The most common gains were detected at chromosomes 19q (6 of 12, 50%), 16p (5 of 12, 41.6%), 12q (5 of 12, 41.6%), 10q (5 of 12, 41.6%), 11p (4/of 12, 33.3%), 4p (3 of 12, 25%), and 8q (3/12, 25%). The most

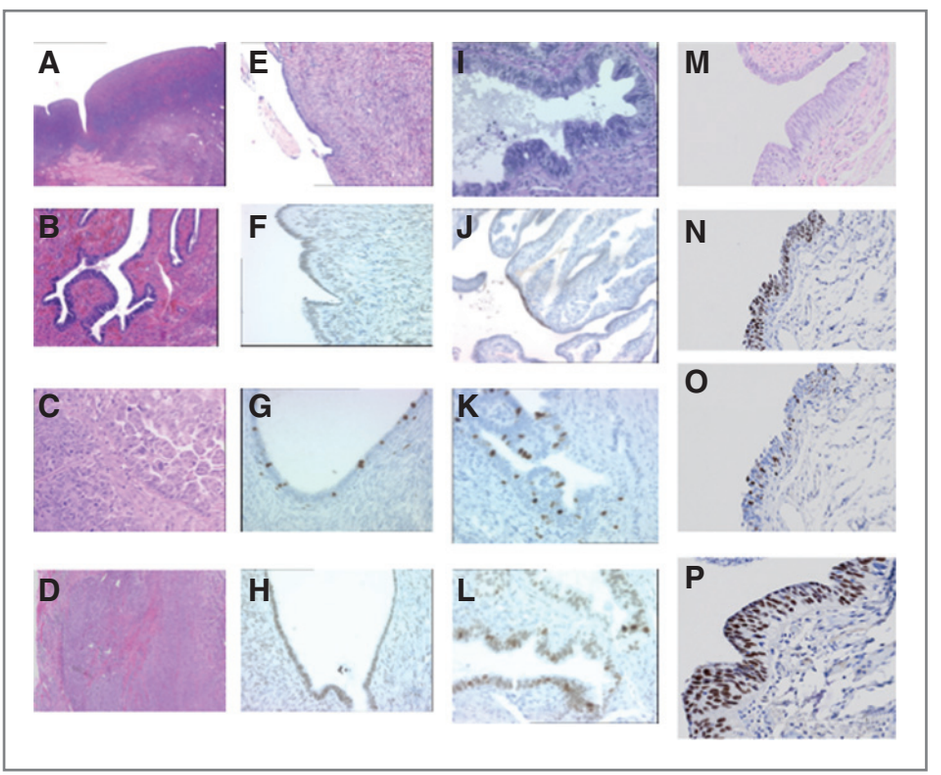

Figure 3. Representative hematoxylin and eosin (H&E)-stained and immunostained sections. A, normal control ovary (H&E); B, normal control fallopian tube (H&E); C, serous ovarian cancer (H&E); D, tubal cancer (H&E); E, ovarian dysplasia (H&E); F, p53 immunopositivity in ovarian dysplasia; G, Ki67 immunopositivity in ovarian dysplasia; H, high γH2AX immunopositivity in ovarian dysplasia; I, tubal dysplasia (H&E); J, p53 immunopositivity in tubal dysplasia; K, Ki67 immunopositivity in tubal dysplasia; L, high γH2AX immunopositivity in tubal dysplasia; M, STIC (H&E); N, strong p53 immunopositivity in STIC; O, Ki67 immunopositivity in STICs; P, strong γH2AX immunopositivity in STICs.

Downloaded from clincancerres.aacrjournals.org on September 20, 2020. © 2013 American Association for Cancer Research.

Published OnlineFirst April 15, 2013; DOI: 10.1158/1078-0432.CCR-12-3947

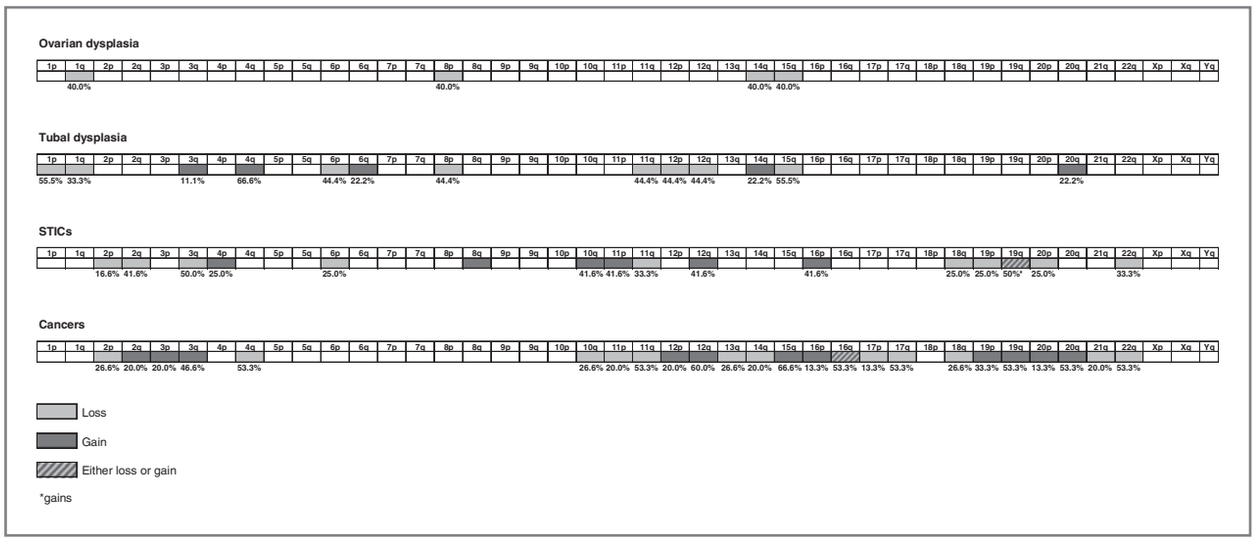

Figure 4. aCGH results: the common genomic gains and losses found in dysplasia, STIC, and cancer groups.

common losses were at chromosomes 3q (6 of 12, 50%), 2q (5 of 12, 41.6%), 11q (4 of 12, 33.3%), 6p (4 of 12, 33.3%), 22q (4 of 12, 33.3%), 18q (3 of 12, 25%), 19p (3 of 12, 25%), 20p (3 of 12, 25%), and 2p (2 of 12, 16.6%). The size of rearrangements in STICs was also greater than for dysplasia samples, with an average of 2,363.37 kb (488–8,161). The minimal regions of interest in the common losses and gains are given in Supplementary Table S3.

aCGH results for cancer samples. Finally, the alterations were the greatest in terms of both size (8,726 kb, 946–74,650) and number (20.3, 10–41; Figs. 4 and 5). The most common gains were detected at chromosomes 15q (10 of 15, 66.6%), 12q (9 of 15, 60%), 16q (8 of 15, 53.3%), 19q (8 of 15, 53.3%), 3q (7 of 15, 46.6%), 19p (5 of 15, 33.3%), 20q (5 of 15, 33.3%), 12p (3 of 15, 20%), 3p (3 of 15, 20%), 2q (3 of 15, 20%), 20p (2 of 15, 13.3%), and 16p (2 of 15, 13.3%). The most common losses were at chromosomes 11q (8 of 15, 53.3%), 16q (8 of 15, 53.3%), 17q (8 of 15, 53.3%), 22q(8 of 15, 53.3%), 4q (7 of 15, 53.3%), 10q (4 of 15, 26.6%), 13q (4 of 15, 26.6%), 18q (4 of 15, 26.6%), 2p (4 of 15, 26.6%), 11p (3 of 15, 20%) 14q (3 of 15, 20%), 21q (3 of 15, 20%), and 17p (2 of 15, 13.3%).

Discussion

We have revealed telomere shortening and chromosomal rearrangements in the potential precursors of ovarian cancer: TOD and STICs, indicative of genomic instability. TODs and STICs have shorter telomeres than noncancerous controls. High-grade serous ovarian cancer telomeres are shorter than noncancerous controls but longer than TOD and STIC precursors. The correlation of telomeres shortening with the BRCA gene status and activation of proteins involved in DNA damage response (γH2AX) provide additional evidence for the existence of genomic instability in these preinvasive conditions.

Telomeres are located at the extremity of the chromosomes and consist of multiple hexameric repeats 5′-TTAGGG-3′. Their main function is to ensure chromosome stability. Telomeres are regularly shortened during cell division. The critical shortening ("telomere crisis") results

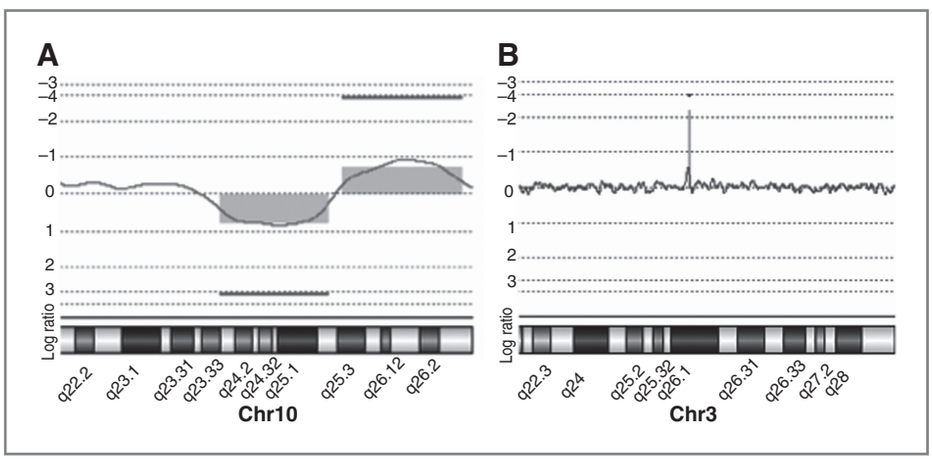

Figure 5. Examples of aCGH results for ovarian cancer (A) and tubal dysplasia (B) patients showing deletion and amplification on chromosome 10q and 3q. aCGH chromosome views show log ratio profile for the aberrant areas of chromosome 10q (A) and 3q (B). Vertical axis indicates gain or loss of genome copy number and horizontal axis indicates the physical position on chromosome.

Downloaded from clincancerres.aacrjournals.org on September 20, 2020. © 2013 American Association for Cancer Research.

Published OnlineFirst April 15, 2013; DOI: 10.1158/1078-0432.CCR-12-3947

in chromosomal instability, activation of the DNA repair processes, then cellular death. In tumors the telomeres are usually shortened, rendering the chromosomes instable, without reaching the critical length which results in cell death, activation of telomerase, which is able to regenerate telomeres, generally limited to stem cells, progenitor cells, and tumor cells, but not present in normal somatic cells, enables the continuous proliferation of genetically unstable cancer cells (15–17).

Telomere dysfunction has been described as one of the first phases in genomic instability (29–31). Telomere shortening appears to take place in most human preinvasive epithelial lesions: telomeres shorten in 88% of early precancerous conditions of the bladder, cervix, colon, esophagus, or prostate (15, 32).

Telomerase activation probably takes place later during the invasive stage and would thus counterbalance the telomere shortening: stabilization of the telomere length at this stage would moreover represent an advantage in terms of tumor proliferation and escaping apoptosis (16).

In our study, STIC samples showed the shortest telomeres, in agreement with the results of Kuhn and colleagues (22), followed by dysplasia and then cancer samples. So there appears to be a gradual shortening of telomeres during transition from dysplasia to STIC phase. Given that STICs have the shortest telomeres, they could be in a telomere crisis phase preceding genomic stabilization due to telomerase activation. Analysis of the expression of telomerase would most probably help to confirm this hypothesis.

In dysplasia group, no difference was found in terms of telomere length according to the type of organ (ovary or tube). However, a significant difference appeared between the BRCA1 and BRCA2 mutation statuses (the TOD was even more unstable when there was a BRCA1 type mutation). The BRCA1 and 2 genes play a key role in DNA signaling and repair (33): BRCA1, BRCA2 (via hRAD51), and p53 interact in cooperation in the DNA repair (mainly by homologous recombination). DNA repair does not take place in mice with BRCA1 mutation: the result is activation of p53 and cell-cycle arrest (34). So a BRCA1 mutation would contribute to enhanced instability (35).

BRCA1 and 2 were shown to be telomere-modifying genes. BRCA1 may regulate telomeres by multiple mechanisms, including regulation of telomerase activity and additional telomerase-independent mechanisms related to 3′ G-strand telomeric overhang length and possibly also to telomere degradation (36). BRCA2-mediated homologous recombination reactions contribute to the maintenance of telomere length by facilitating telomere replication (37, 38). An association between shorter telomeres in peripheral blood leucocytes and increased risk of ovarian cancer, particularly for younger women, was reported in families carrying BRCA1/2 mutations as well as in sporadic cases (39). Our data suggest that BRCA1 mutations might have greater impact on telomere shortening than BRCA2 mutations in both ovarian and tubal dysplasia, and further studies are necessary to confirm this finding and to investigate possible underlying mechanisms. BRCA1 gene seems to be involved in multiple telomere maintenance mechanisms, which could perhaps explain that its deficiency has stronger impact on the telomere length, at least in ovarian and tubal tissue.

The telomere length of normal individuals is high heterogeneous. The variation in the T/S ratios observed in controls is most likely related to various degree of degradation of DNA obtained from microdissected fixed tissue samples. In the case of peripheral blood, it was noted that T/S ratios were higher in dried blood spots, which may be partially degraded, than in freshly obtained blood samples (40). In our study, samples from control, dysplasia, and cancer tissues were collected and extracted in exactly the same way, and this similarity of sample treatment enabled us to compare the results.

High expression of γH2AX (surrogate marker of genetic instability signaling double-stranded breaks in DNA) has been evidenced in most human precancerous lesions (40, 41). Experimental studies have shown that H2AX-knockout mice were at greater risk of immune deficiency, infertility and were also more sensitive to ionizing radiation, all of which can be explained by increased chromosomal instability related with decreased efficiency of the DNA repair. When these mice were also knockouts for p53, the risk of developing tumors was also increased (42, 43). Recent studies have also revealed activation of the DNA damage responses in most early precancerous conditions in humans (44, 45).

In our study, we found strong expression of γH2AX in cases of TOD. Concerning STICs, strong and diffuse nuclear marking was found to be present. Finally, telomere dysfunction caused by telomere shortening was strongly correlated with overexpression of γH2AX.

These results prove that DNA repair mechanisms are activated in these early conditions and are definitely an additional indication of genomic instability.

Our final molecular approach to the genomic instability inherent to these early lesions was a global analysis of DNA copy number gains and losses using aCGH (46, 47). In sporadic cancers of the ovary, the rearrangements most frequently found are located in regions 1q, 2p, 2q, 3q, 6q, 7q, 8q, 12p, 17q, 18q, 20q, ch X for gains and in ch4, 6q, 8p, 13q, 16q, 18q, Xq for losses (48). It has even been shown that these profiles are distinctly different between sporadic ovarian cancers and ovarian cancers of a hereditary type due to BRCA mutation (49–51): genomic imbalances appear to be more numerous in case of genetic risk, probably because there is less DNA repair (one of the functions of BRCA) and the genome is thus more fragile.

So in hereditary ovarian cancers related with BRCA mutations, very frequent chromosome amplifications at 1q, 2q, 3q, and 8q along with deletions at 9q and a chromosome 19 were often found (49–51). CGH thus allows specific molecular profiles to be established. Moreover amplifications and deletions may include tumor suppressors and oncogenes. Different pathways involving kinase function, cell-cycle regulation, or apoptosis could be significantly affected. Genomic profiles may help to molecularly subtype cancers

Downloaded from clincancerres.aacrjournals.org on September 20, 2020. © 2013 American Association for Cancer Research.

Published OnlineFirst April 15, 2013; DOI: 10.1158/1078-0432.CCR-12-3947

and lead toward individualized cancer-type–specific therapies as it has been shown with the Cancer Genome Atlas (52–54).

Yet there are no data of this nature concerning precancerous ovarian conditions: we postulated that CGH could target particular regions involved in the early stages of ovarian carcinogenesis. We found an increase in terms of both number and size between dysplasia lesions and STICs, confirming that genetic instability already exists in these very early stages (55).

It has even been shown that these profiles are distinctly different between sporadic ovarian cancers and ovarian cancers of a hereditary type due to BRCA mutation (49–51). And yet these secondary rearrangements—probably responsible for continued proliferation and the metastatic risk—do not necessarily have any direct link with the pathogenesis and tumorigenesis. The Cancer Genome Atlas project (54) has shown that high-grade serous ovarian cancers are characterized by TP53 mutations in 96% of all tumors as it is the case in STICSs. However, other additional mutated genes with low prevalence have been shown in ovarian cancers (BRCA1, BRCA2, NF1, RB1, CDK12, CSMD3, FAT3, GABRA6), and we did not find them in our precancerous lesions. Conversely, the early alterations in precancerous lesions are certainly key stages in these initial phases of carcinogenesis, and the corresponding candidate genes could act directly in tumor initiation and represent targets for diagnosis and/or treatment. Some authors (50, 51) underline, for example, the importance of the long arm of chromosome 11 which carries several genes encoding for DNA repair proteins (such as *γH2AX*): we did indeed find deletions at 11q not only in dysplasia but also in STICs. In our dysplasia series, certain rearrangements encompass genes involved in the DNA repair system and/or the transcription and regulation channels for various cytokines [*hLMB1* or *ING4* involved in the *p53* signaling pathway at *12 p13.31*, *MIM135A2* at *12q23.1*, *RAG1*, *RAG2*, *C11orf74* at *11p12*, *PTHLH* at *12p11.23*, *DOK5* at *14q32.2-q32.33*, *TRAF3* at *20q13.2*, ITGB3BP (co-activator of retinoic nuclear receptors) at *1p31.3*]. In STICs, rearrangements detected in the present study contain genes involved in transcriptional or translational regulation (*MEIS1* at *2p24*, *NCK1* at *3q26.2-q26.31*, *GAK* at *4p16.3*, *MIR202* at *10q26.3*) as well as genes involved in the regulation of DNA damage response (OLA1 at *2q31.1-q31.2*, *RAD21* at *8q13.1-q24.3*) and apoptosis (*GAK* at *4p16.3* and *AXIN1* at *16p13.3*). Other studies are needed to confirm the involvement of these gene candidates by considering regions common to cases of dysplasia, STICs and cancers (*at 3q, 11q at 12q*) as priority targets.

The parallel with breast cancer and its precursor lesions is suggestive: recurrent genomic changes have been found in well-differentiated ductal carcinoma *in situ* (CIS) including loss of 16q and gain in 1q. Poorly differentiated CIS have shown more recurrent changes as the gains in 1q, 5p, 8q, chromosome 17, and the losses in 8p, 11q, 13q, and 14q (46). Some authors have even shown a probable clonal relationship between CIS and invasive cancers due to the existence of identical chromosomal abnormalities in both cases (56).

In addition, specific profiles have been discovered that differ between hereditary and sporadic forms of breast cancer. Certain regions that are amplified (3q, 20q) or deleted (5q) and the corresponding genes (*TM4SF1*, *BCAS4*, *RAD50*) found in hereditary type tumors would suggest defects in the DNA repair system with a consequent installation of genomic instability (46, 56–58).

Ovarian/tubal dysplasia and STIC showed breakpoints in telomeric bands (Supplementary Tables). In particular, ovarian and tubal dysplasia had a common terminal breakpoint at chromosome 14q32.33. Tubal dysplasia had another telomeric breakpoint at 12q24.33. Among the frequent breakpoints in STICs, more than half occurred at terminal bands: 4p16.3; 8q24.3; 10q26.3, 11p15.5, 12q24.33; 16p13.3; 19q13.43; 20p13; and 22g13.33. This is in line with the study by Gisselsson and colleagues (59), showing the clustering of breakpoints at telomeric chromosomal bands at initial stages of genomic instability in cancer. These data also confirm that cells from STICs, which are characterized by the shortest telomeres, are undergoing a telomere crisis with the occurrence of end-to-end telomere fusions and breakage fusion bridge cycles involving many chromosomes.

By using CGH technique, it is not possible to take into account reorganizations or rearrangements of the genome. This technique only can envisage genome unbalances such as gains, losses, or amplification events. Unfortunately, array CGH analyses for genome-wide chromosomal imbalance using paraffin sections is a limitation because large amounts of DNA are required (60). This is why we were unable to analyze all the samples extracted from small ovarian and tubal epithelium specimens. These are therefore preliminary results and will need to be confirmed in larger cohorts. The next step will consist of screening and identification of the genes corresponding to the regions revealed by CGH array along with study of the correlation between telomere length and activation of telomerase.

Disclosure of Potential Conflicts of Interest

No potential conflicts of interest were disclosed.

Authors' Contributions

Conception and design: G. Chene, J. Dauplat, F.P. Llorca
Development of methodology: G. Chene, A. Tchirkov, E. Pierre-Eymard, F.P. Llorca
Acquisition of data (provided animals, acquired and managed patients, provided facilities, etc.): G. Chene, A. Tchirkov, E. Pierre-Eymard, I. Raoelfils, A. Cayre, E. Watkin, P. Vago, F.P. Llorca
Analysis and interpretation of data (e.g., statistical analysis, biostatistics, computational analysis): G. Chene, A. Tchirkov, E. Pierre-Eymard, I. Raoelfils, A. Cayre, E. Watkin, P. Vago, F.P. Llorca
Writing, review, and/or revision of the manuscript: G. Chene, A. Tchirkov, E. Pierre-Eymard, J. Dauplat, I. Raoelfils, A. Cayre, E. Watkin, P. Vago, F.P. Llorca
Administrative, technical, or material support (i.e., reporting or organizing data, constructing databases): A. Tchirkov, E. Pierre-Eymard, I. Raoelfils, A. Cayre, E. Watkin, P. Vago
Study supervision: J. Dauplat, F.P. Llorca

Downloaded from clincancerres.aacrjournals.org on September 20, 2020. © 2013 American Association for Cancer Research.

Published OnlineFirst April 15, 2013; DOI: 10.1158/1078-0432.CCR-12-3947

Acknowledgments

The authors thank Farida Godeau, Mathieu Roche, and Christiane Jullien for technical assistance and Lorraine Gameiro from Centre Imagerie Cellulaire Santé (CICS, Clermont-Ferrand, France) for her help with laser microdissection.

The costs of publication of this article were defrayed in part by the payment of page charges. This article must therefore be hereby marked *advertisement* in accordance with 18 U.S.C. Section 1734 solely to indicate this fact.

Received December 30, 2012; revised March 25, 2013; accepted March 27, 2013; published OnlineFirst April 15, 2013.

References

1. Negrini S, Gorgoulis VG, Halazonetis TD. Genomic instability, an evolving hallmark of cancer. Nat Rev Moll Cell Biol 2010;11:220–8.
2. Lengauer C, Kinzler KW, Vogelstein B. Genetic instability in colorectal cancers. Nature 1997;386:623–27.
3. Folkins AK, Jarboe EA, Saleemuddin A, Lee Y, Callahan MJ, Drapkin R, et al. A candidate precursor to pelvic serous cancer (p53 signature) and its prevalence in ovaries and fallopian tubes from women with BRCA mutations. Gynecol Oncol 2008;109:168–73.
4. Kindelberger D, Lee Y, Hirsch MS, Feltmate D, Medeiros F, Callahan MJ, et al. Intraepithelial carcinoma of the fimbria and pelvic serous carcinoma: evidence for a causal relationship. Am J Surg Pathol 2007;31:161–9.
5. Powell CB, Kenley E, Chen LM, Crawford B, McLennan J, Zaloudek C, et al. Risk-reducing salpingo-oophorectomy in BRCA mutation carriers: role of serial sectioning in the detection of occult malignancy. J Clin Oncol 2005;23:127–32.
6. Finch A, Shaw P, Rosen B, Murphy J, Narod SA, Colgan TJ. Clinical and pathologic findings of prophylactic salpingo-oophorectomies in 159 BRCA1 and BRCA2 carriers. Gynecol Oncol 2006;100:58–64.
7. Medeiros F, Muto MG, Lee Y, Elvin JA, Callahan MJ, Feltmate C, et al. The tubal fimbria is a preferred site for early adenocarcinoma in women with familial ovarian cancer syndrome. Am J Surg Pathol 2006;30:230–6.
8. Crum CP. Intercepting pelvic cancer in the distal fallopian tube: theories and realities. Mol Oncol 2009;3:165–70.
9. Mehrad M, Ning G, Chen EY, Mehra KK, Crum CP. A pathologist's road map to benign, precancerous, and malignant intraepithelial proliferations in the Fallopian tube. Adv Anat Pathol 2010;17:293–302.
10. Gross AL, Kurman RJ, Vang R, Shih IM, Visvanathan K. Precursor lesions of high-grade serous ovarian carcinoma: morphological and molecular characteristics. J Oncol 2010;2010:126295.
11. Piek JM, van Diest PJ, Zweemer RP. Dysplastic changes in prophylactic removed fallopian tubes of women predisposed to developing ovarian cancer. J Pathol 2001;195:451–6.
12. Deligdisch L, Gil J, Kerner H, Wu HS, Beck D, Gershoni-Baruch R. Ovarian dysplasia in prophylactic oophorectomy specimens. Cancer 1999;86:1544–50.
13. Deligdisch L. Ovarian dysplasia: a review. Int J Gynecol Cancer 1997;7:89–94.
14. Lee Y, Miron A, Drapkin R, Nucci MR, Medeiros F, Saleemuddin A, et al. A candidate precursor to serous carcinoma that originates in the distal fallopian tube. J Pathol 2007;211:26–35.
15. Artandi SE, DePinho RA. Telomeres and telomerase in cancer. Carcinogenesis 2010;31:9–18.
16. Svenson U, Roos G. Telomere length as a biological marker in malignancy. Biochim Biophys Acta 2009;1792:317–23.
17. Kruk PA, Godwin AK, Hamilton TC, Auersperg N. Telomeric instability and reduced proliferative potential in ovarian surface epithelial cells from women with a family history of ovarian cancer. Gynecol Oncol 1999;73:229–36.
18. Chene G, Penault-Llorca F, Le Bouedec G, Dauplat MM, Mishellany F, Jaffeux P, et al. Ovarian epithelial dysplasia and prophylactic oophorectomy for genetic risk. Int J Gynecol Cancer 2009;19: 65–72.
19. Schlosshauer PW, Cohen CJ, Penault-Llorca F, Miranda CR, Bignon YJ, Dauplat J, et al. Prophylactic oophorectomy: a morphologic and immunohistochemical study. Cancer 2003;98:2599–606.
20. Dauplat J, Chene G, Pomel C, Dauplat MM, Le Bouedec G, Mishellany F, et al. Comparison of dysplasia profiles in stimulated ovaries and in those with a genetic risk for ovarian cancer. Eur J Cancer 2009;45: 2977–83.
21. Chene G, Dauplat J, Raoelfils I, Bignon Y J, Cayre A, Jaffeux P, et al. Ovarian epithelial dysplasia: description of a dysplasia scoring scheme. Ann Pathol 2011;31:3–10.
22. Kuhn E, Meeker A, Wang TL, Sehdev AS, Kurman RJ, Shih IM. Shortened telomeres in serous tubal intraepithelial carcinoma: an early event in ovarian high-grade serous carcinogenesis. Am J Surg Pathol 2010;34:829–36.
23. Hu CY, Taymor ML, Hertig AT. Primary carcinoma of the fallopian tube. Am J Obstet Gynecol 1950;59:58–67.
24. Sedlis A. Carcinoma of the fallopian tube. Surg Clin North Am 1978;58:121–9.
25. Espina V, Milia J, Wu G, Cowherd S, Liotta LA. Laser capture microdissection. Methods Mol Biol 2006;319:213–29.
26. Domazet B, MacLennan GT, Lopez-Beltran A, Montironi R, Cheng L. Laser capture microdissection in the genomic and proteomic era: targeting the genetic basis of cancer. Int J Clin Exp Pathol 2008;1:475–88.
27. Cawthon RM. Telomere measurement by quantitative PCR. Nucleic Acid Res 2002;30:1–6.
28. Richard M. Cawthon. Telomere length measurement by a novel monochrome multiplex quantitative PCR method. Nucl Acids Res 2009; 37:e21.
29. Johnson KL, Dukes KA, Vidaver J, LeShane ES, Ramirez I, Weber WD, et al. Interlaboratory comparison of fetal male DNA detection from common maternal plasma samples by real-time PCR. Clin Chem 2004;50:516–21.
30. Lengauer C, Kinzler KW, Vogelstein B. Genetic instabilities in human cancers. Nature 1998;396:643–49.
31. Vollebergh MA, Jonkers J, Linn SC. Genomic instability in breast and ovarian cancers: translation into clinical predictive biomarkers. Cell Moll Life Sci 2012;69:223–45.
32. Meeker AK, Hicks JL, Platz EA, March GE, Bennett CJ, Delannoy MJ, et al. Telomere shortening is an early somatic DNA alteration in human prostate tumorigenesis. Cancer Res 2002;62:6405–9.
33. Jazaeri AA, Yee CJ, Sotiriou C, Brantley KR, Boyd J, Liu ET. Gene expression profiles of BRCA1-linked, BRCA-2linked, and sporadic ovarian cancers. J Natl Cancer Inst 2002;94:990–1000.
34. Brugarolas J, Jacks T. Double indemnity: p53, BRCA, and cancer. Nat Med 1997;3:721–22.
35. Chene G, Dauplat J, Radosevic-Robin N, Cayre A, Penault-Llorca F. Tu-be or not tu-be: that is the question. . .About serous ovarian carcinogenesis. Crit Rev Oncol Hematol. Epub 2013 Mar 21.
36. Ballal RD, Saha T, Fan S, Haddad BR, Rosen EM. BRCA1 localization to the telomere and its loss from the telomere in response to DNA damage. J Biol Chem 2009;284:36083–98.
37. Badie S, Escandell JM, Bouwman P, Carlos AR, Thanasoula M, Gallardo MM, et al. BRCA2 acts as a RAD51 loader to facilitate telomere replication and capping. Nat Struct Mol Biol 2010;17:1461–9.
38. Martinez-Delgado B, Yanowsky K, Inglada-Perez L, de la Hoya M, Caldes T, Vega A, et al. Shorter telomere length is associated with increased ovarian cancer risk in both familial and sporadic cases. J Med Genet 2012;49:341–4.
39. Zanet DL, Saberi S, Oliveira L, Sattha B, Gadawski I, Côté HC. Blood and dried blood spot telomere length measurement by qPCR: assay considerations. PLoS One 2013;8:e57787.
40. Mah LJ, El-Osta A, Karagiannis TC. γH2AX as a molecular marker of aging and disease. Epigenetics 2010;2:129–36.
41. Clingen PH, Wu JYH, Miller J, Mistry N, Chin F, Wynne P, et al. Histone H2AX phosphorylation as a molecular pharmacological marker for DNA interstrand crosslink cancer chemotherapy. Bioch Pharmacol 2008;76:19–27.

Downloaded from clincancerres.aacrjournals.org on September 20, 2020. © 2013 American Association for Cancer Research.

Published OnlineFirst April 15, 2013; DOI: 10.1158/1078-0432.CCR-12-3947

42. Bassing CH, Suh H, Ferguson DO, Chua KF, Manis J, Eckersdorff M, et al. Histone H2AX: a dosage-dependent suppressor of oncogenic translocations and tumors. Cell 2003;114:359–70.
43. Celeste A, Difilippantonio S, Difilippantonio MJ, Fernandez-Capetillo O, Pilch DR, Sedelnikova OA, et al. H2AX haploinsufficiency modifies genomic stability and tumor susceptibility. Cell 2003;114:371–83.
44. Gorgoulis VG, Vassiliou LV, Karakaidos P, Zacharatos P, Kotsinas A, Liloglou T, et al. Activation of the DNA damage checkpoint and genomic instability in human precancerous lesions. Nature 2005;434:907–13.
45. Bartkova J, Horejsí Z, Koed K, Krämer A, Tort F, Zieger K, et al. DNA damage response as a candidate anti-cancer barrier in early human tumorigenesis. Nature 2005;434:864–70.
46. Climent J, Garcia JL, Mao JH, Arsuaga J, Perez-Losada J. Characterization of breast cancer by array comparative genomic hybridization. Biochem Cell Biol 2007;85:497–508.
47. Davies JJ, Wilson IM, Lam WL. Array CGH technologies and their applications to cancer genomes. Chromosome Res 2005;13:237–48.
48. Fishman A, Shalom-Paz E, Fejgin M, Gaber E, Altaras M, Amiel A. Comparing the genetic changes detected in the primary and secondary tumor sites of ovarian cancer using comparative genomic hybridization. Int J Gynecol Cancer 2005;15:261–6.
49. Hu J, Khanna V, Jones MW, Surti U. Comparative study of primary and recurrent ovarian serous carcinomas: comparative genomic hybridization analysis with a potential application for prognosis. Gynecol Oncol 2003;89:369–75.
50. Israeli O, Gotlieb WH, Friedman E, Goldman B, Ben-Baruch G, Aviram-Goldring A, et al. Familial vs sporadic ovarian tumors: characteristic genomic alterations analyzed by CGH. Gynecol Oncol 2003;90:629–36.
51. Bruchim I, Israeli O, Mahmud SM, Aviram-Goldring A, Rienstein S, Friedman E, et al. Genetic alterations detected by comparative genomic hybridization and recurrence rate in epithelial ovarian carcinoma. Cancer Genet Cytogenet 2009;190:66–70.
52. Wrzeszczynski KO, Varadan V, Byrnes J, Lum E, Kamalakaran S, Levine DA, et al. Identification of tumor suppressors and oncogenes from genomic and epigenetic features in ovarian cancer. PLoS One 2011;6:e28503.
53. Beroukhim R, Mermel CH, Porter D, Wei G, Raychaudhuri S, et al. The landscape of somatic copy-number alteration across human cancers. Nature 2010;463:899–05.
54. Bell D, Berchuck A, Birrer M, Chien J, Cramer DW, et al. Integrated genomic analyses of ovarian carcinoma. Nature 2011;474:609–15.
55. Salvador S, Rempel A, Soslow RA, Gilks B, Huntsman D, Miller D. Chromosomal instability in fallopian tube precursor lesions of serous carcinoma and frequent monoclonality of synchronous ovarian and fallopian tube mucosal serous carcinoma. Gynecol Oncol 2008;110:408–17.
56. Waldman FM, De Vries S, Chew KL, Moore DH, Kerlikowske K, Ljung BM. Chromosomal alterations in ductal carcinomas in situ and their in situ recurrences. J Natl Cancer Inst 2000;92:313–20.
57. van Beers EH, van Welsem T, Wessels LSA. Comparative genomic hybridization profiles in human BRCA1 and BRCA2 breast tumors highlight differential sets of genomic aberrations. Cancer Res 2005;65:822–7.
58. Srefansson OA, Jonasson JG, Johannsson OT, Olafsdottir K, Steinarsdottir M, Valgeirsdottir S, et al. Genomic profiling of breast tumours in relation to BRCA abnormalities and phenotypes. Breast Cancer Res 2009;11:1–14.
59. Gisselsson D, Jonson T, Petersen A, Strombeck B, Dal Cin P, Hoglund M, et al. Telomere dysfunction triggers extensive DNA fragmentation and evolution of complex chromosome abnormalities in human malignant tumors. PNAS 2001;98:12683–8.
60. Huang J, Pang J, Watanabe T, Ng HK, Ohgaki H. Whole genome amplification for array comparative genomic hybridization using DNA extracted from formalin-fixe, paraffin-embedded histological sections. J Mol Diagn 2009;11:109–16.

Downloaded from clincancerres.aacrjournals.org on September 20, 2020. © 2013 American Association for Cancer Research.

Published OnlineFirst April 15, 2013; DOI: 10.1158/1078-0432.CCR-12-3947

AACR American Association for Cancer Research

Clinical Cancer Research

Early Telomere Shortening and Genomic Instability in Tubo-Ovarian Preneoplastic Lesions

Gautier Chene, Andrei Tchirkov, Eleonore Pierre-Eymard, et al.

Clin Cancer Res 2013;19:2873-2882. Published OnlineFirst April 15, 2013.

Updated version	Access the most recent version of this article at: doi:10.1158/1078-0432.CCR-12-3947
Supplementary Material	Access the most recent supplemental material at: http://clincancerres.aacrjournals.org/content/suppl/2013/04/17/1078-0432.CCR-12-3947.DC1

Cited articles	This article cites 59 articles, 8 of which you can access for free at: http://clincancerres.aacrjournals.org/content/19/11/2873.full#ref-list-1
Citing articles	This article has been cited by 6 HighWire-hosted articles. Access the articles at: http://clincancerres.aacrjournals.org/content/19/11/2873.full#related-urls

E-mail alerts	Sign up to receive free email-alerts related to this article or journal.
Reprints and Subscriptions	To order reprints of this article or to subscribe to the journal, contact the AACR Publications Department at pubs@aacr.org.
Permissions	To request permission to re-use all or part of this article, use this link http://clincancerres.aacrjournals.org/content/19/11/2873. Click on "Request Permissions" which will take you to the Copyright Clearance Center's (CCC) Rightslink site.

Downloaded from clincancerres.aacrjournals.org on September 20, 2020. © 2013 American Association for Cancer Research.